EUROPEAN ORGANIZATION FOR NUCLEAR RESEARCH

CERN-EP/89-161
12 December 1989

GAS MIXTURES FOR TRANSITION RADIATION DETECTORS AT HIGH-LUMINOSITY COLLIDERS

B. Dolgoshein*), M. Potekhin,
A. Romanyuk and V. Sosnovtsev

Moscow Physical Engineering Institute, USSR

ABSTRACT

The electron drift velocities in xenon with admixtures of CO_2 and CF_4 were measured with the aid of a cylindrical proportional chamber. The spectroscopy characteristics and ageing problems of such chambers are discussed.

(Submitted to Nuclear Instruments and Methods in Physics Research)

*) Visitor at CERN, Geneva, Switzerland.

1. INTRODUCTION

It is a well-established fact that much of the interesting physics to be studied at future colliders (SSC, LHC, UNK) is mostly accessible through the study of leptonic channels (e, μ, ν). The observation of transition radiation (TR) can provide valuable *non-destructive* information for lepton identification, which is both complementary and supplementary to calorimetric measurements.

The gas mixture to be used in the proportional chambers of transition radiation detectors (TRDs) for future colliders [1, 2] must

i) provide high drift velocities of ionization electrons;

ii) contain an optimal concentration of xenon in order to enhance the rejection power of a TRD;

iii) provide high detector vitality, i.e. suppress ageing processes that are mainly due to polymerization on the anodes.

Analysis of up-to-date information on electron drift velocities in Xe-containing mixtures [3–7], as well as information on ageing problems, allowed us to choose two molecular admixtures—CO_2 and CF_4—as the most promising candidates for satisfying conditions (i) and (iii).

Our calculations give 1.6–2.0 mm as the optimal effective Xe thickness in TRD proportional chambers.

We have measured the electron drift velocity and other characteristics of different Xe mixtures.

2. TESTING DEVICE

A schematic layout of the device is shown in fig. 1. It consists of a triggering part and a measuring cell. The UV beam of a pulsed laser is split in two by means of a semitransparent mirror: 95% of the beam goes into the measuring cell and 5% goes directly to the photodiode. The measuring cell has two flat disk electrodes of 60 mm diameter, with 5 mm spacing between them. A cylindrical proportional chamber is embedded in the lower electrode, and its anode, made of gold-plated tungsten wire, is parallel to the electrode plane.

When the upper electrode (photocathode) is lit by the laser flash, some 10^3 electrons are liberated from its surface. After drifting 5 mm they enter the proportional chamber volume through a gap of 0.8 mm width. The gas gain is about 5×10^3–10^4.

The anode signal is amplified by a fast current amplifier and fed to the input 'B' of the two-channel oscilloscope. The gas gain is monitored with a ^{55}Fe γ-source (5.95 keV).

The oscillogram pattern is shown in fig. 2. We can see two signals from the fast amplifier. The first one corresponds to photoelectrons from the walls of the cylindrical chamber, which are produced by laser radiation scattered within the cell. The time coordinate of this signal matches the collection time of the electrons within the chamber. The second signal is given by the electrons that have drifted all the way from the upper electrode (photocathode) of the cell.

The device described above made it possible to measure the total electron collection time in cylindrical proportional chambers of 4 and 5 mm diameter, and for different anode diameters (20–100 μm), with 1 ns precision, as well as to measure electron drift velocities in the range 0.2–10.0 kV/cm with 5% precision.

3. MAIN RESULTS

We have measured the following characteristics of gas mixtures:

1) drift velocities of electrons in Xe with admixtures of CO_2 and of CF_4;
2) the electron collection time for these mixtures at Xe partial pressures of 0.4, 0.5, and 0.6 atm;
3) the amplitude of signals and the spectroscopy properties for these mixtures.

3.1 Drift velocities

In figs. 3 and 4, the electron drift velocities for Xe + CO_2 mixtures are plotted versus E/p. For mixtures of Xe + CO_2 the dependence has a kind of plateau above 6 kV/cm. For Xe + CF_4 mixtures, the drift velocity falls steeply in a large field after reaching a maximum.

Figure 5 shows the dependence of the signal amplitude on the drift field value (i.e. the field in the drift region between the upper and lower electrodes). In a high electric field there is a reduction of the number of electrons. This phenomenon is a consequence of an established process of dissociative electron capture,

$$e + CF_4 \rightarrow F + CF_3^- \ ,$$

which reveals a peak at an electron energy of $\sim$ 4 eV [8].

3.2 Collection time

Figures 6 to 12 show the dependence of the collection time on the admixture percentage. The electron collection time was measured using the cylindrical proportional chambers with 4 and 5 mm cathode diameter, at a gas gain of $\sim 10^4$ (anode diameters from 20 to 100 μm). The xenon pressure chosen was such that the effective partial Xe

length would correspond to 1.6–2.0 mm at normal pressure [0.4–0.5 atm (absolute) of Xe for a 5 mm cathode, and 0.5–0.6 atm for a 4 mm cathode].

It follows from the data that in a 4 mm diameter proportional chamber at 1 atm, an absolute total collection time of 34 ns is viable with Xe (50%) + CO_2 (50%), whilst with Xe (50%) + CF_4 (50%) the time is 30 ns.

3.3 Spectroscopy characteristics

Figure 13 shows the pulse-height spectra for a 5 mm diameter chamber irradiated by a ^{55}Fe γ-source (5.95 keV). The anode diameter was 70 μm, the gas gain 5 $\times 10^3$. The Xe + CO_2 gas mixture has an energy resolution of 22% FWHM, whereas the 'fast' mixture, Xe + CF_4, has a rather poor resolution, about 60% FWHM. This deterioration of the resolution is mainly due to the dissociative capture of electrons, as mentioned above, a process that works effectively in the anode region.

4. AGEING

As was shown in ref. [6], the values of the charge dose, after which the chambers show signs of ageing, are

$$\sim 0.5\text{–}1.0 \text{ C/cm for rare gases + } CO_2 \ ,$$

$$\geq 5 \text{ C/cm for mixtures with } CF_4 \ .$$

Both values are an order of magnitude larger than the total annual charge foreseen when running at the SSC [1]. At the LHC the situation will be more difficult.

We are now planning to carry out the experimental measurements of ageing properties under realistic conditions.

5. CONCLUSION

In a 4 mm diameter proportional chamber filled with the mixture Xe (50%) + molecular additive (50%) it is possible to obtain 34 ns collection time with CO_2 and 30 ns with CF_4. Nevertheless the Xe + CO_2 mixture seems to be preferable because, although it is just slightly slower than Xe + CF_4, it has the following advantages:

i) a better energy resolution, which might be significant for amplitude measurements in TRDs [1];

ii) CO_2 is two times less dense than CF_4, which diminishes the dE/dx of ionizing particles and so improves the rejection power of TRDs;

iii) the presence of a plateau in the drift velocity dependence allows us to anticipate a close to linear dependence of the spatial coordinate on time. This is important for track-position measurements with small-diameter (so-called 'straw') proportional chambers of transition radiation detectors [1].

REFERENCES

[1] B. Dolgoshein, Proc. ECFA Study Week on Instrumentation for High-Luminosity Hadron Colliders, Barcelona, 1989 (CERN 89–10, ECFA 89–124, Geneva, 1989), Vol. 2, p. 650.

[2] J. Schank et al., TRD and tracker for the SSC, private communication.

[3] H. Daum et al., Nucl. Instrum. Methods **152** (1978) 541.

[4] A. Peisert and F. Sauli, report CERN 84–08 (1984).

[5] L.G. Christophorou et al., Nucl. Instrum. Methods **171** (1980) 491.
J. Fisher, V. Radeka and G. Smith, Nucl. Instrum. Methods **A246** (1986) 511.

[6] J. Va'vra, Nucl. Instrum. Methods **A252** (1986) 547.

[7] S. Majewski et al., same Proceedings as ref. [1], Vol. 1, p. 239.

[8] L.G. Christophorou et al., Nucl. Instrum. Methods **163** (1979) 141.

Figure captions

Fig. 1: Schematic view of the apparatus for measuring the characteristics of gas mixtures.

Fig. 2: Time measurements with an oscilloscope.

Fig. 3: The dependence of the electron drift velocity in Xe + CO_2 mixtures, on the electric field.

Fig. 4: The dependence of the electron drift velocity, in Xe + CF_4 mixtures, on the electric field.

Fig. 5: The dependence of the signal pulse height on the electric field in the drift region (photoelectrons from a laser pulse).

Fig. 6–12: The dependences of total electron collection time on molecular admixture concentrations for different cathode and anode diameters and different xenon pressures (abs.).

Fig. 13: Pulse-height spectra from a cylindrical proportional chamber irradiated with ^{55}Fe ($E_\gamma = 5.95$ keV), at a gas gain of 5×10^3 for different Xe mixtures.

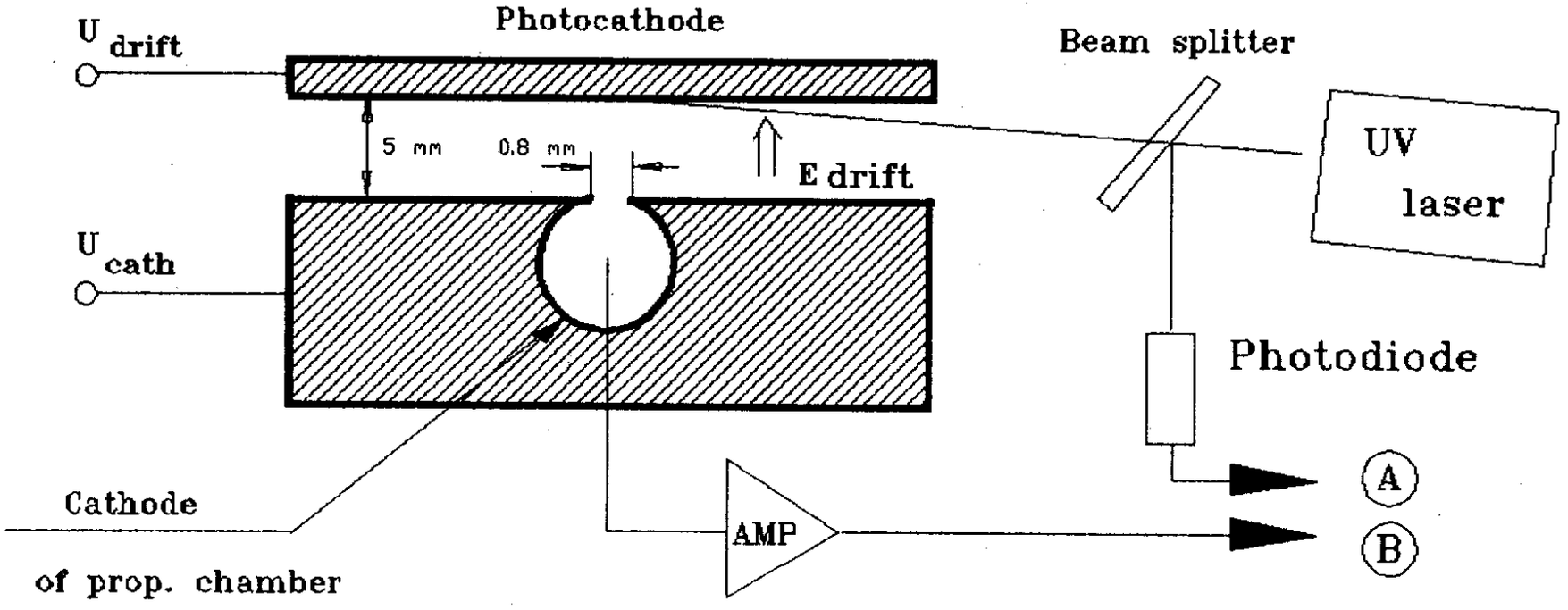
U drift
Photocathode
Beam splitter
UV
laser
5 mm
0.8 mm
E drift
U cath
Photodiode
Cathode
of prop. chamber
AMP
A
B

Fig. 1

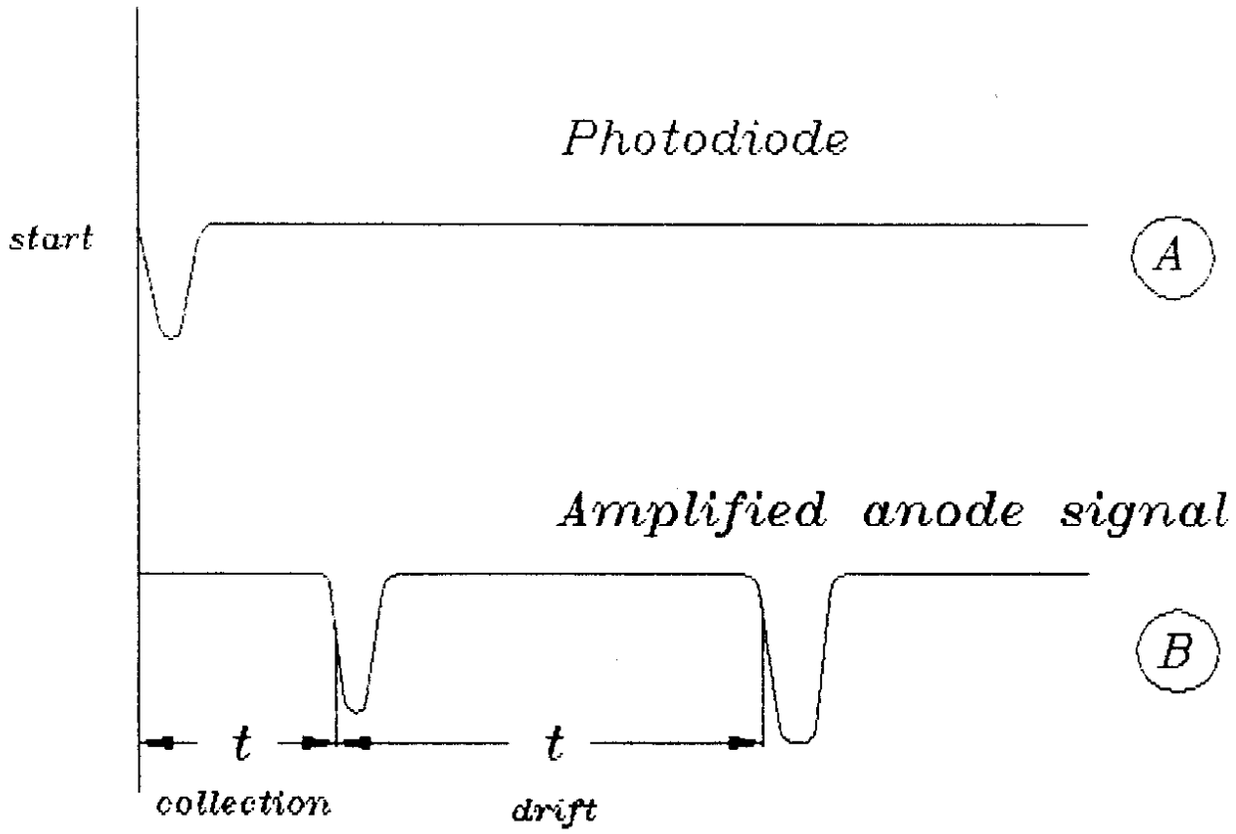
Oscillogram pattern
Photodiode
start
A
Amplified anode signal
B
t
t
collection
drift

Fig. 2

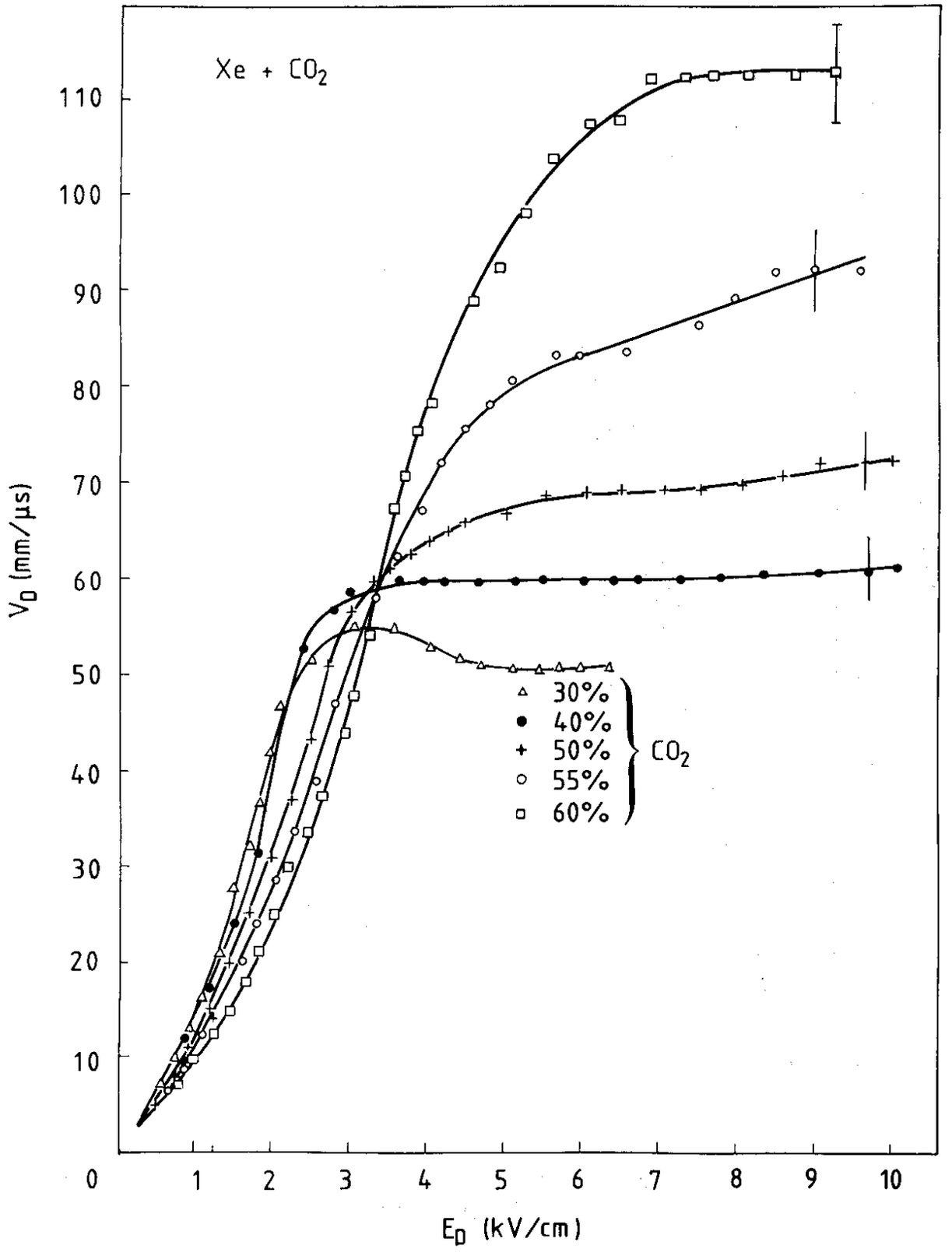
Xe + CO2
110
100
90
80
70
60
50
40
30
20
10
0
1
2
3
4
5
6
7
8
9
10
VD (mm/μs)
ED (kV/cm)
30%
40%
50%
55%
60%
CO2

Fig. 3

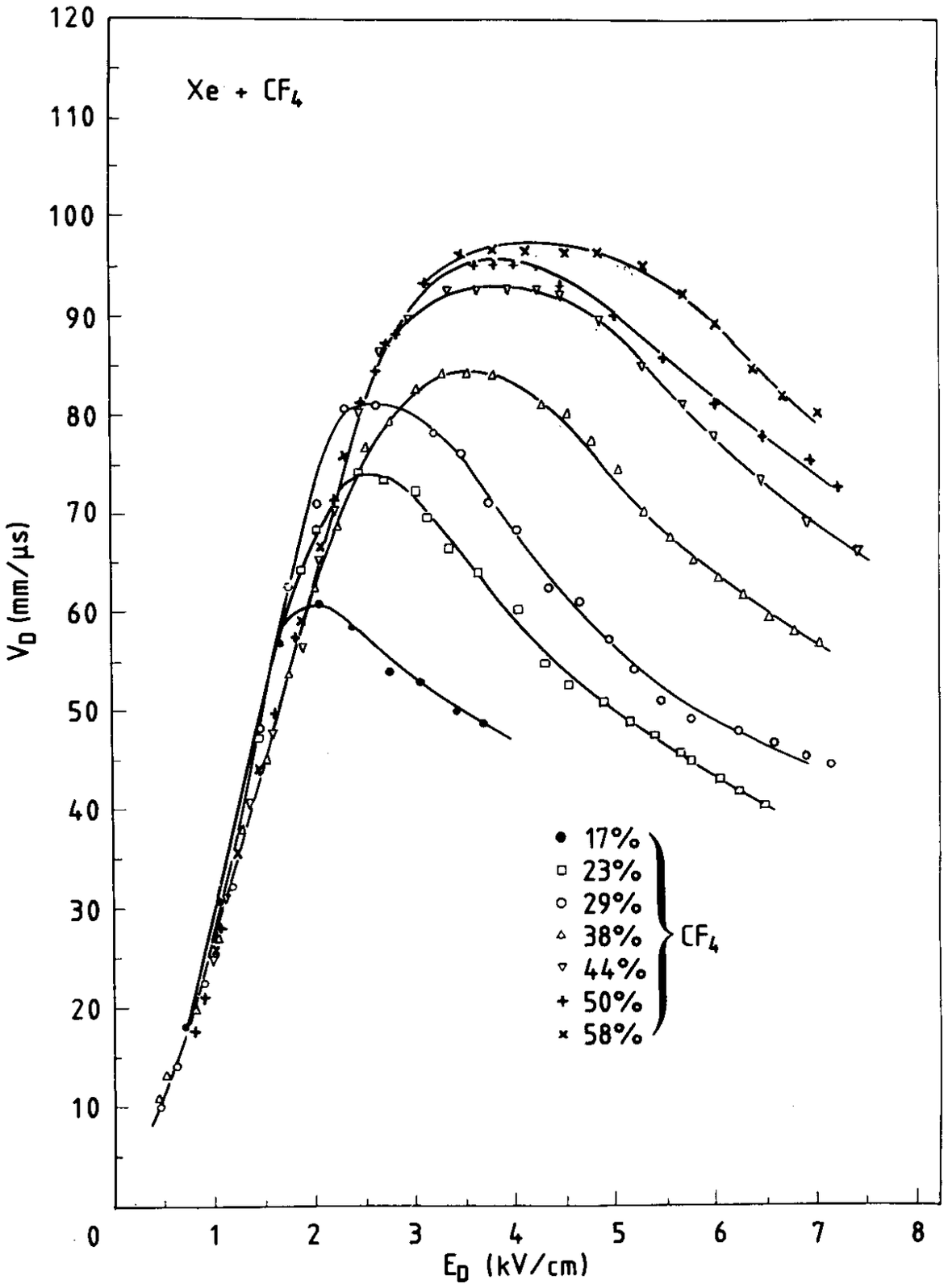
Xe + CF4
120
110
100
90
80
70
60
50
40
30
20
10
0
1
2
3
4
5
6
7
8
VD (mm/µs)
ED (kV/cm)
17%
23%
29%
38%
44%
50%
58%
CF4

Fig. 4

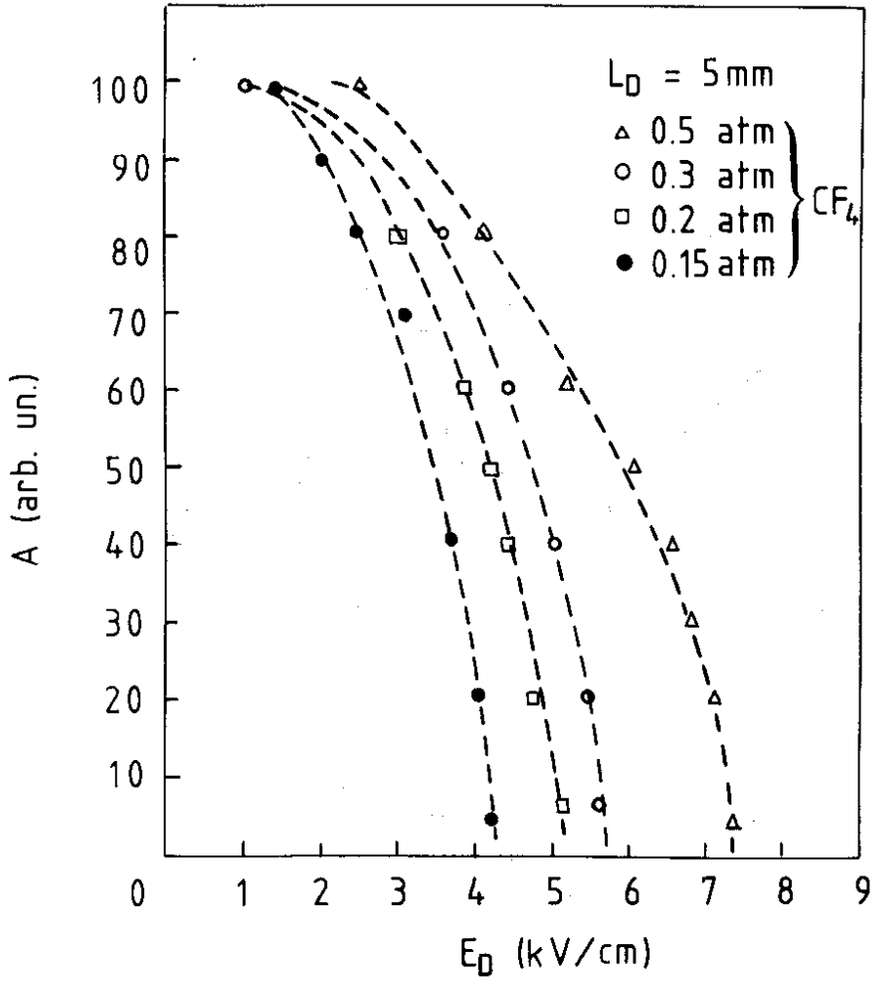
A (arb. un.)
E_D (kV/cm)
L_D = 5 mm
0.5 atm
0.3 atm
0.2 atm
0.15 atm
CF_4

Fig. 5

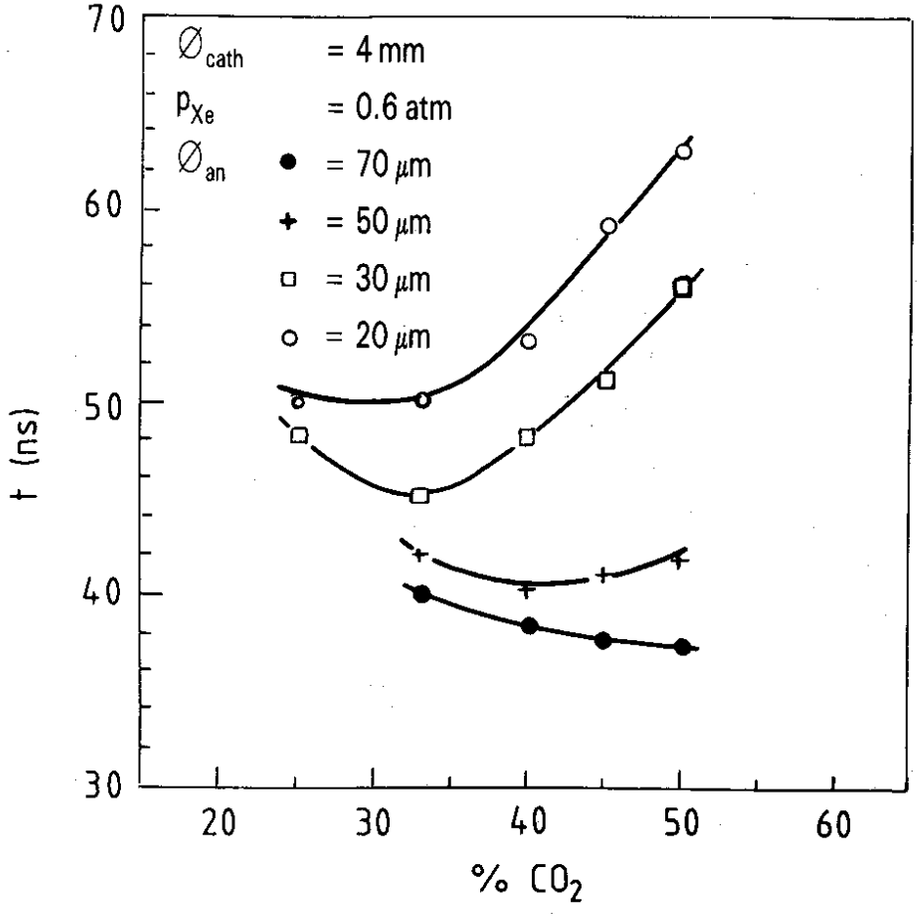
t (ns)
% CO_2
$\varnothing_{cath}$ = 4 mm
p_{Xe} = 0.6 atm
$\varnothing_{an}$
= 70 μm
= 50 μm
= 30 μm
= 20 μm

Fig. 6

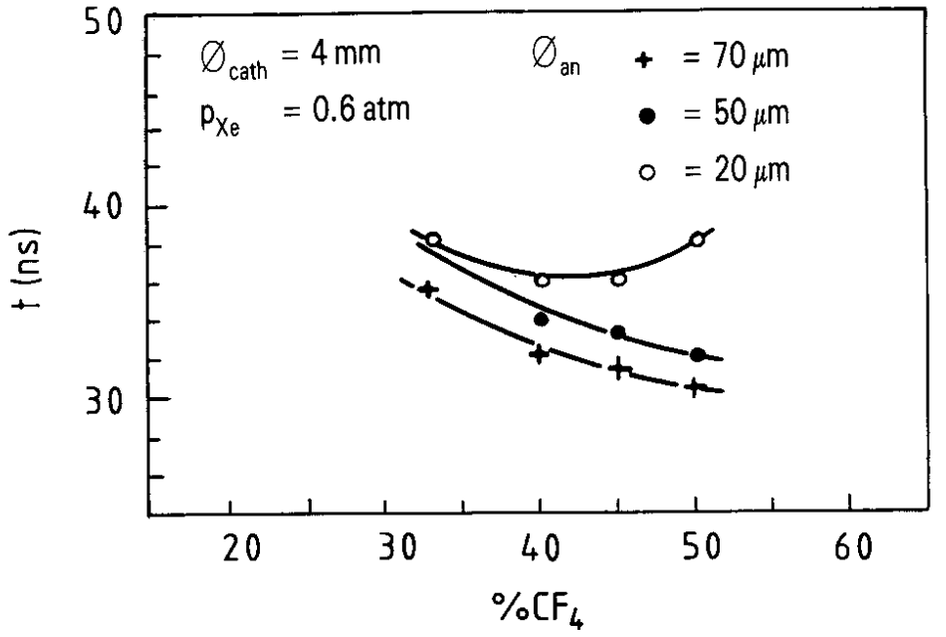
50
40
30
t (ns)
$\varnothing_{cath}$ = 4 mm
p_{Xe} = 0.6 atm
$\varnothing_{an}$
+ = 70 μm
● = 50 μm
○ = 20 μm
20
30
40
50
60
%CF_4

Fig. 7

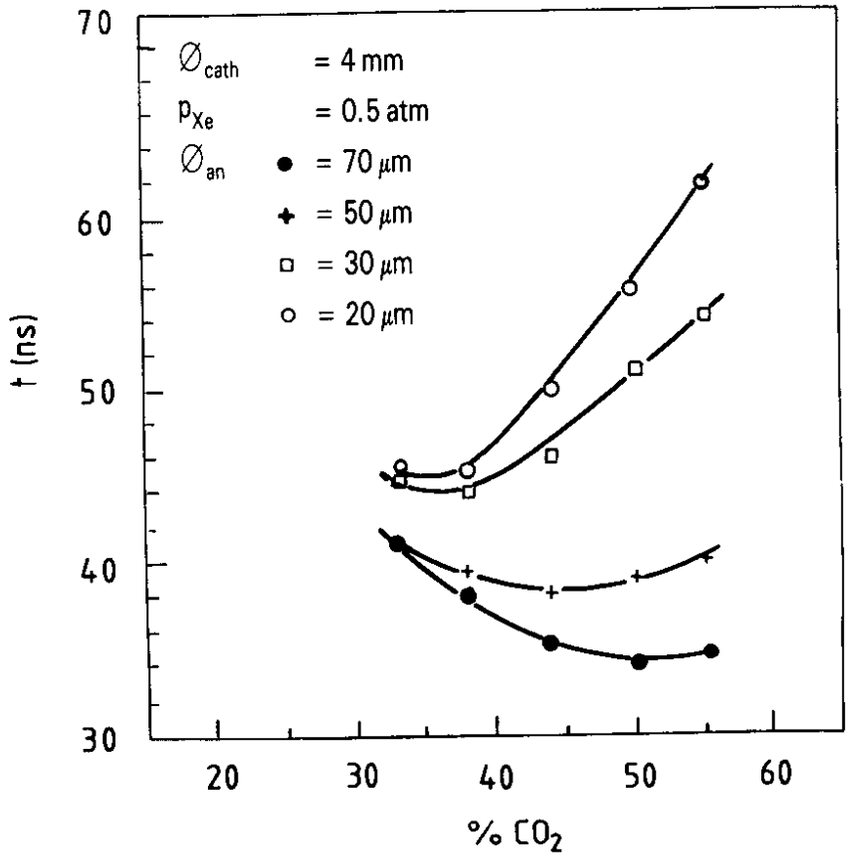
70
60
50
40
30
t (ns)
$\varnothing_{cath}$ = 4 mm
p_{Xe} = 0.5 atm
$\varnothing_{an}$
● = 70 μm
+ = 50 μm
□ = 30 μm
○ = 20 μm
20
30
40
50
60
% CO_2

Fig. 8

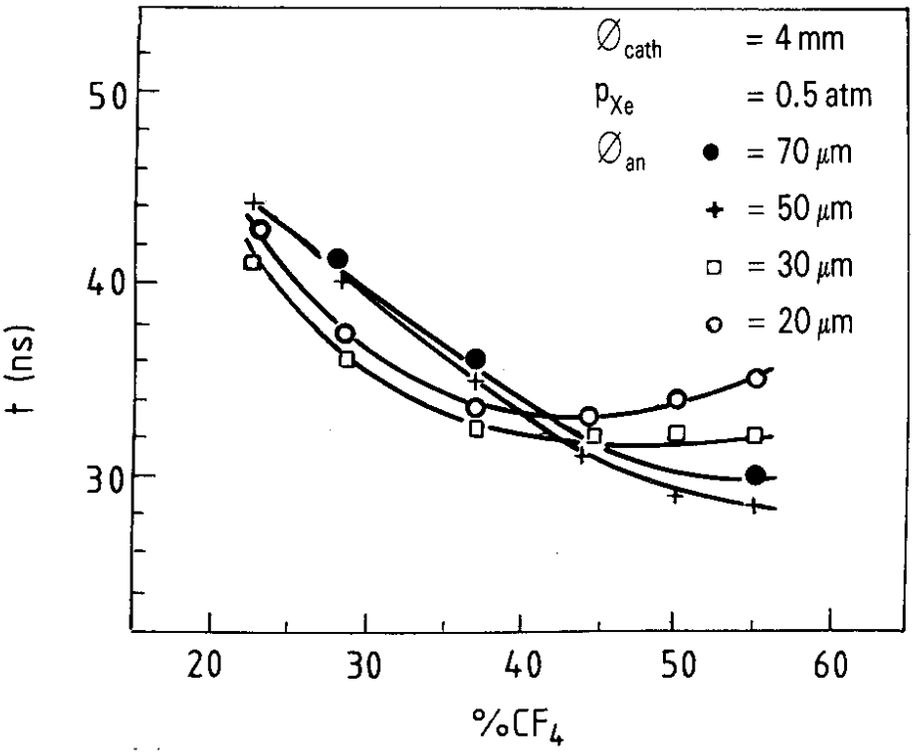
$\varnothing_{cath}$ = 4 mm
p_{Xe} = 0.5 atm
$\varnothing_{an}$
● = 70 μm
+ = 50 μm
□ = 30 μm
○ = 20 μm
50
40
30
t (ns)
20
30
40
50
60
%CF_4

Fig. 9

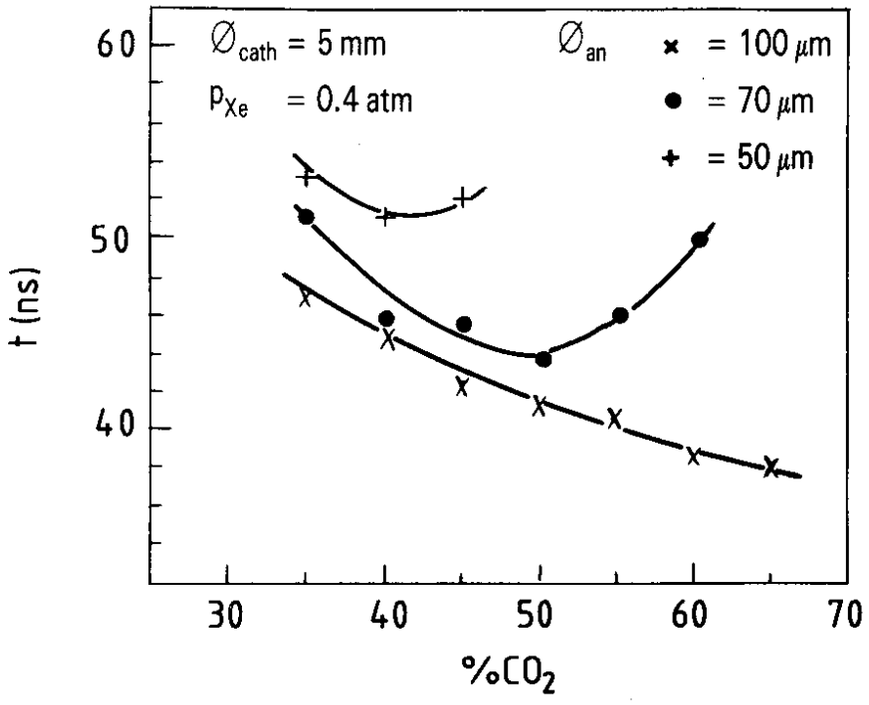
$\varnothing_{cath}$ = 5 mm
p_{Xe} = 0.4 atm
$\varnothing_{an}$
× = 100 μm
● = 70 μm
+ = 50 μm
60
50
40
t (ns)
30
40
50
60
70
%CO_2

Fig. 10

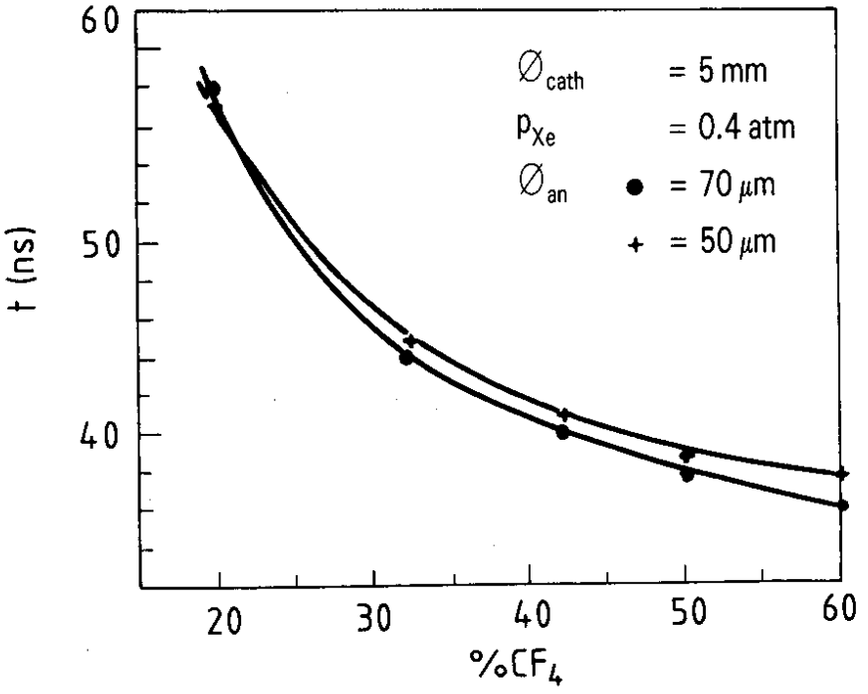
60
50
40
t (ns)
$\varnothing_{cath}$ = 5 mm
p_{Xe} = 0.4 atm
$\varnothing_{an}$ ● = 70 μm
+ = 50 μm
20
30
40
50
60
%CF_4

Fig. 11

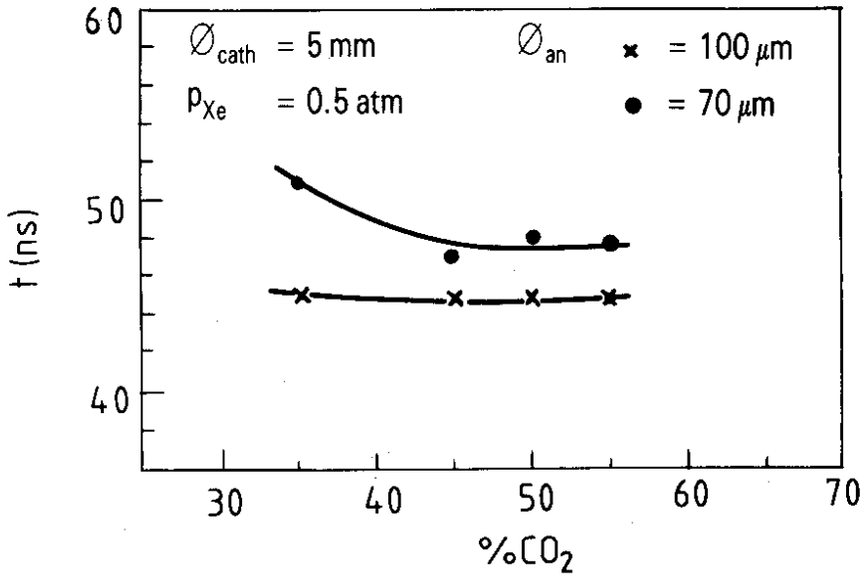
60
50
40
t (ns)
$\varnothing_{cath}$ = 5 mm
p_{Xe} = 0.5 atm
$\varnothing_{an}$ × = 100 μm
● = 70 μm
30
40
50
60
70
%CO_2

Fig. 12

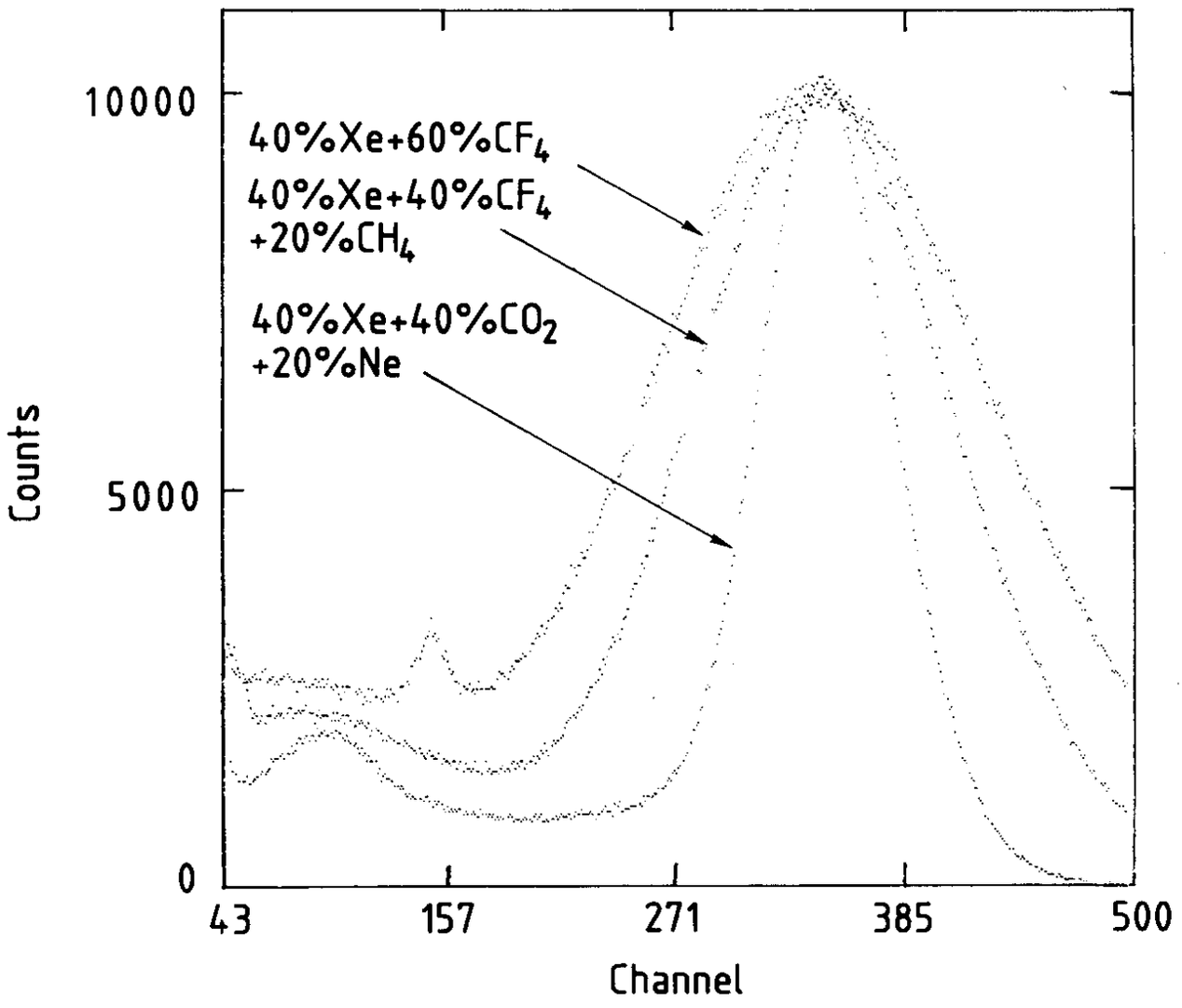
10000
5000
0
Counts
40%Xe+60%CF4
40%Xe+40%CF4
+20%CH4
40%Xe+40%CO2
+20%Ne
43
157
271
385
500
Channel

Fig. 13